4

Ensemble Averaging and Resolution Enhancement of Digital Radar and Sonar Signals

Leiv Øyehaug[1*] and Roar Skartlien[2*]
[1]*Centre of Integrative Genetics and Department of Mathematical Sciences and Technology, Norwegian University of Life Sciences,*
[2]*Institute of Energy Technology, Department of Process and Fluid Flow Technology, Norway*

1. Introduction

In radar and sonar signal processing it is of interest to achieve accurate estimation of signal characteristics. Recorded pulse data have uncertainties due to emitter and receiver noise, and due to digital sampling and quantization in the receiver system. It is therefore important to quantify these effects through theory and experiment in order to construct "smart" pulse processing algorithms which minimize the uncertainties in estimated pulse shapes. Averaging reduces noise variance and thus more accurate signal estimates can be achieved. Considering a signal processing system that involves sampling, A/D-conversion, IQ-demodulation and ensemble averaging, this chapter forms a theoretical basis for the statistics of ensemble averaged signals, and summarizes the basic dependencies on bit-resolution, ensemble size and signal-to-noise ratio.

Repetitive signals occur in radar and sonar processing, but also in other fields such as medicine (Jane et al., 1991; Schijvenaars et al, 1994; Laguna & Sornmo, 2000) and environment monitoring (Viciani et al., 2008). Practical ensemble averaging is subject to alignment error (jitter) (Meste & Rix, 1996), but we will neglect this effect. The effective bit-resolution of the system can be increased by ensemble averaging of repetitive, A/D-converted signals, provided that the signal contains noise (Belchamber & Horlick, 1981; Ai & Guoxiang, 1991; Koeck, 2001; Skartlien & Øyehaug, 2005).

Due to varying radar and sonar cross section for scattering objects, or varying antenna gain of a sweeping emitter or receiver, the pulses exhibit variation in scaling. In the case of radar or sonar, the cross section of the target may then vary from pulse to pulse, but not appreciably over the pulse width. The scanning motion of the radar antenna may also affect the pulse scaling regardless of the target model, but we can safely neglect the time variation of the scaling due to this effect. In the case of a passive sensor, the signal propagates from an unknown radar emitter to the sensor antenna, and there is no radar target involved. Only

[*] The present study was conceived of and initiated during the authors' employment with the Norwegian Defence Research Establishment, P.O. Box 25, 2027 Kjeller, Norway.

Source: Advances in Sonar Technology, Book edited by: Sergio Rui Silva,
ISBN 978-3-902613-48-6, pp. 232, February 2009, I-Tech, Vienna, Austria

the scanning motion of the emitter antenna (and possibly the sensor antenna) may in this case influence the scaling. In general, we assume that the scaling can be treated as a random variable accounted for by a given distribution function (Øyehaug & Skartlien, 2006).
In the present chapter we briefly review some of the theory of ensemble averaging of quantized signals in absence of random scaling (Sect. 2) and summarize results on ensemble averaging of randomly scaled pulses (in absence of quantization) modulated into amplitude and phase (Sect. 3). Aided by numerical simulations, we subsequently extend the results of the preceding sections to amplitude and phase modulations of scaled, quantized pulses (Sect. 4). In Sect. 5 we discuss how the theoretical results can be implemented in practical signal processing scenarios and outline some of the issues that still require clarification. Finally, in Sect. 6 we draw conclusions.

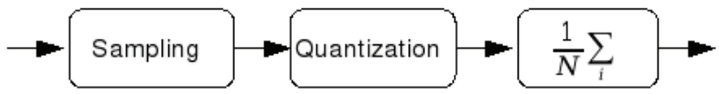

Fig. 1. The signal chain considered in Sect. 2. After sampling, the signal is quantized (A/D-converted) followed by ensemble averaging.

2. Ensemble averaging of quantized signals; benefitting from noise

This section considers the statistical properties of ensemble averages of quantized, sampled signals (Fig. 1), and demonstrates that the expectation of the quantization error diminishes with increasing noise, at the cost of a larger error variance. As the ensemble average approximates the expectation, it follows that the quantization error (in the ensemble average) can be made much smaller than what corresponds to the bit resolution of the system. We will also demonstrate that there is an optimum noise level that minimizes the combined effect of quantization error and noise. First, consider a basic analog signal with additive noise;

$$y_i(t) = s(t) + n_i(t), \tag{1}$$

where t is time, and n is random noise. We observe N realizations of y, and the index i denotes one particular realization i (or sonar or radar pulse i). We assume that s is repetitive (independent of i), while n varies with i. We assume a general noise distribution function with zero mean and variance σ^2. The recorded signal is sampled at discrete t_j giving $y_{i,j}$, and these samples are subsequently quantized through a function Q to obtain the sampled and A/D-converted digital signal $x_{i,j} = Q(y_{i,j})$. We consider the quantization to be uniform, i.e. the separation between any two neighboring quantization levels is constant and equal to Δ. The probability distribution function (pdf) of $x_{i,j}$ is discrete and generally asymmetric even if the pdf of n is continuous and symmetric.

2.1 Error statistics

We define the error in the quantized signal as $e_{i,j} = x_{i,j} - s_j$ accounting for both noise and quantization effects. The noise in different samples is uncorrelated and we assume that the

correlation time is sufficiently small such that the noise between different time-samples is also uncorrelated.

To illuminate the effect of ensemble averaging, we consider the one-bit case for which the quantizer has two levels: 0 and 1. If the input is larger than 1/2 the output will be 1, otherwise the output is 0. Consider a constant "signal" $s_j = 1/2$. For zero noise the output is always 1, giving an error of 1/2. If we introduce noise with a symmetric pdf with zero mean, the quantizer output "flips" between 0 and 1 randomly. The expectation value of the output is then 1/2, since we expect an equal number of zeroes and ones on the output, hence the expectation value of the error is zero. If the input signal is larger or smaller than 1/2, there will be an error such that the expected error of the output is nonzero.

For Gaussian noise combined with a uniform quantizer with many levels, Carbone and Petri (1994) derived

$$E[e_{i,j};s_j] = \frac{\Delta}{\pi}\sum_{k=1}^{\infty}\frac{(-1)^k}{k}\exp[-2\pi^2k^2(\sigma/\Delta)^2]\sin(2\pi k s_j/\Delta). \tag{2}$$

It is easy to see that the expected error is reduced and goes to zero for increasing noise. The reason for this is that for increasing noise, the discrete pdf of the quantized signal becomes an increasingly more accurate representation of the continuous pdf of $y_{i,j}$ (with expectation s_j). The pdf of $y_{i,j}$ gets "broader" and is thus better resolved on the fixed grid defined by the quantizer cells. The expected error attains its largest values for zero noise where it becomes a "sawtooth" function of s_j and, for intermediate noise, it becomes roughly sinusoidal as function of s_j (Fig. 2, left), since only the first few terms in the series expansion are significant.

Along with the expectation value of the error, there is an error variance, defined by $\mathrm{Var}[e_{i,j};s_j] = E[e_{i,j}^2;s_j] - E^2[e_{i,j};s_j]$, which can also be derived in terms of a trigonometric series. For Gaussian noise,

$$E[e_{i,j}^2;s_j] = \frac{\Delta^2}{12} + \sigma^2 + \left(\frac{\Delta}{\pi}\right)^2\sum_{k=1}^{\infty}(-1)^k\left(\frac{1}{k^2} + 4\pi(\sigma/\Delta)^2\right)\exp[-2\pi^2k^2(\sigma/\Delta)^2]\cos(2\pi k s_j/\Delta). \tag{3}$$

It is apparent from the exponential factors that in the large noise limit the error variance goes to $\Delta^2/12 + \sigma^2$ (Fig. 2, right), i.e. the variance is signal-independent. Both a vanishing error expectation, and a variance of σ^2 in the large noise limit, are exactly the properties of the analog signal before quantization.

2.2 Expectation of the sample mean

In the following we consider the ensemble average of $x_{i,j}$,

$$\bar{x}_j = \frac{1}{N}\sum_{i=1}^{N}x_{i,j}. \tag{4}$$

Ensemble averaging has the beneficial effect of reducing the variance, as we expect from basic statistics. Using the asymptotical relations above, one can show that the variance follows the usual $1/N$-law in the large noise limit, i.e. the ensemble average variance goes to

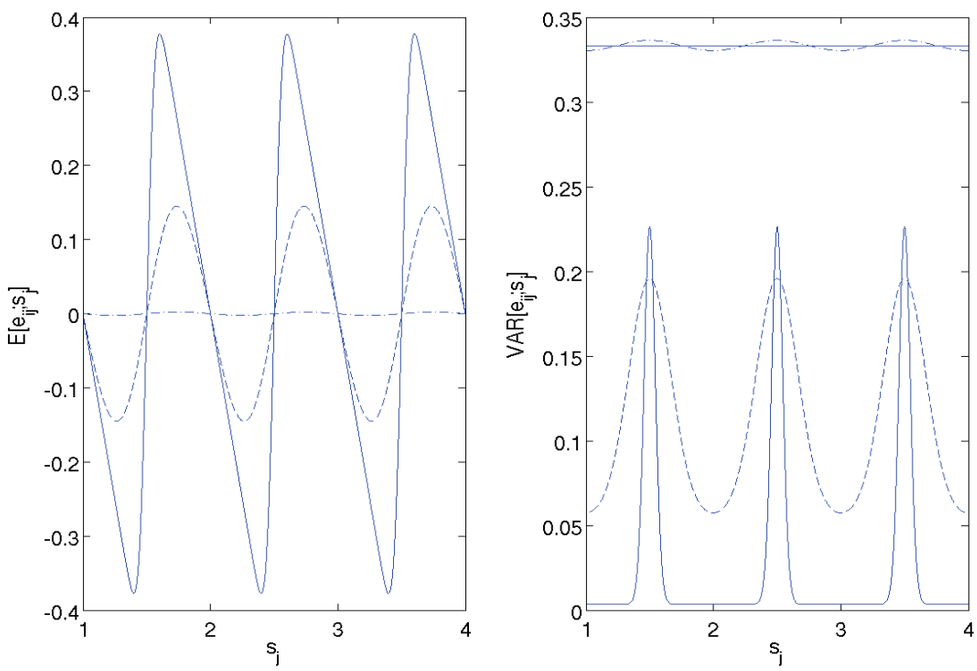

Fig. 2. Signal-dependent expected error (left) and variance (right) for Δ = 1 and three noise levels; σ = 0.05 (full line) σ = 0.2 (dashed) and σ = 0.5 (dash-dotted). In (B), the straight line $\Delta^2/12+\sigma^2$ is plotted to indicate the convergence towards this value with increasing noise.

$\left(\Delta^2/12+\sigma^2\right)/N$ with increasing noise. Thus, the variance of the ensemble average can be made arbitrarily small for increasing ensemble size N. It is important to note that the expectation of the ensemble average converges to the input signal for increasing noise level. Noise is therefore beneficial in this respect, at the cost of a larger variance that can of course be compensated by increasing N.

Furthermore, for small noise, the expectation of the ensemble average differs from the input signal. Ensemble averaging will not remove this difference, since it originates from the deterministic property of the quantizer and not from the noise. We illustrate the effect of noise in Fig. 3, where we compute the average of a sinusoidal with Gaussian noise with variance σ^2 and use a simple roundoff to integer numbers as the quantizer function (i.e. Δ=1). With no noise we obtain a staircase function as expected (Fig. 3, upper panel). With increasing noise, the staircase function is smoothed out to resemble the sine-wave (Fig. 3, lower panels).

2.3 Mean square error (MSE) of the sample mean

With the sample mean as the measured quantity, the associated error is $\bar{e}_j = \bar{x}_j - s_j$. We note that as the sample mean tends to the expectation value as N tends to infinity, $\bar{e}_j$ tends to $E[e_{i,j}]$. For Gaussian noise and for sufficiently large σ/Δ, the mean square error MSE of the sample mean, obtained by averaging $\left(\bar{e}_j\right)^2$ over all discrete samples $j \in [1,...,M]$, is (Skartlien & Øyehaug, 2005),

$$\mathrm{MSE}(\sigma,N) \simeq \frac{1}{N}\left(\sigma^2 + \Delta^2/12\right) + \left(1-\frac{1}{N}\right)\frac{\Delta^2}{2\pi^2}\exp\left(-4\pi^2(\sigma/\Delta)^2\right). \quad (5)$$

When N is given, one can ask what are the bounds on σ to obtain super-resolution? For fixed $N \geq 2$, the requirement $\mathrm{MSE} < \Delta^2/12$ defines the super-resolution interval $(0, \sigma_{\max}(N))$. In the case of Gaussian noise, the upper bound $\sigma_{\max}(N)$ is given implicitly by

$$(N-1)\Delta^2\left(\frac{1}{12} - \frac{1}{2\pi^2}\exp[-4\pi^2(\sigma_{\max}/\Delta)^2]\right) = \sigma_{\max}^2, \quad (6)$$

for large enough σ/Δ. A remarkable property is that there is an optimal noise σ_{opt} in the super-resolution interval $(0, \sigma_{\max}(N))$ which minimizes the MSE. This optimal noise is $\sigma_{\mathrm{opt}} = \Delta\sqrt{\log(2(N-1))/2\pi}$ provided that σ/Δ is sufficiently large and that the noise is Gaussian. For N=100, for example, the optimum value for σ/Δ is close to 0.366, which explains the good averaging performance associated with this value in Fig. 3.

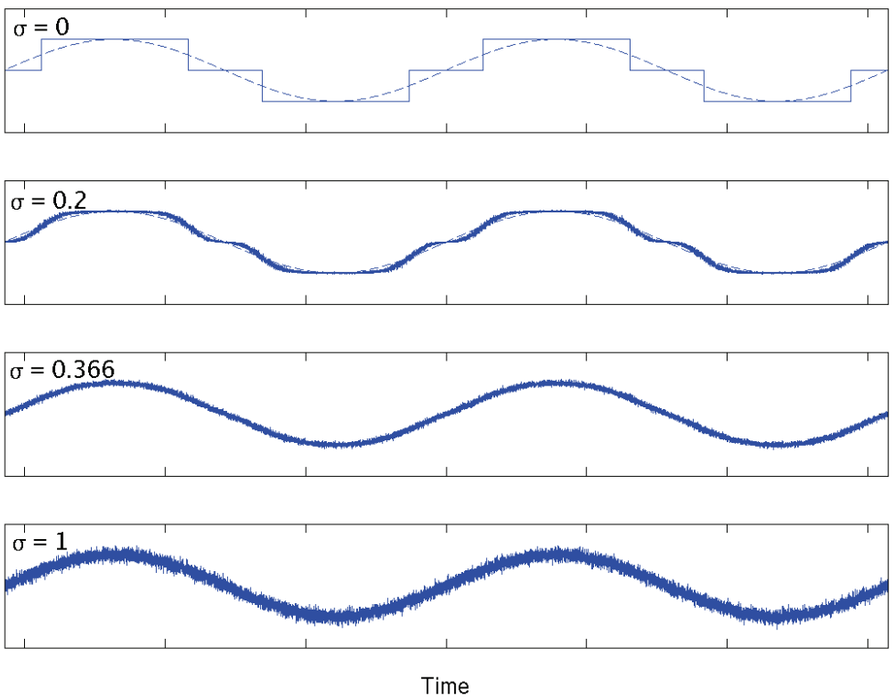

Fig. 3. An example of the effect of ensemble averaging of quantized signals. A sinusoidal with unit amplitude (dashed) plus Gaussian white noise is quantized by a simple roundoff to the nearest integer (i.e. Δ=1) and then averaged over an ensemble of 100 realizations (ensemble average: solid line). In absence of noise we obtain a staircase function (upper panel) and, with increasing noise, the staircase function is smoothed out to resemble the sine-wave. For the particular value σ/Δ=0.366 the mean square error is a minimum.

In summary, the existence of a minimum MSE is a consequence of the balancing between quantizer and noise effects. For small noise ($\sigma < \sigma_{\text{opt}}$), the noise tends to remove the effect from the quantization error in the sample mean and the MSE decreases with increasing noise. For large noise ($\sigma > \sigma_{\text{opt}}$), quantization is roughly negligible compared to the effect of the noise itself, and the MSE increases with increasing noise.

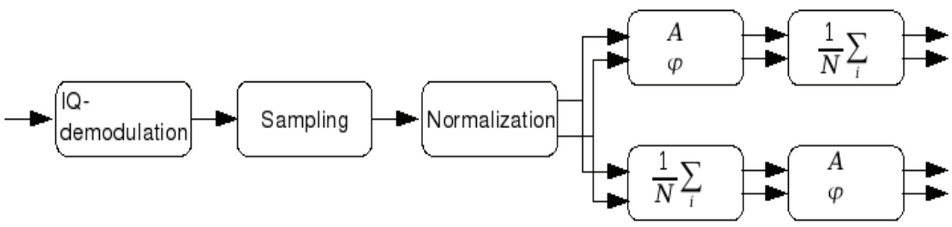

Fig. 4. The signal processing chain considered in Sect. 3. After IQ-demodulation, the signal is sampled and normalized followed by either (i) ensemble averaging of *I* and *Q* and then amplitude/phase modulation (in Sect. 3 referred to as Method I, lower branch) or (ii) amplitude/phase modulation and then ensemble averaging of amplitude and phase (Method II, upper branch).

3. Ensemble averaging of modulated signals that are randomly scaled

In this section our focus is on the statistical properties of the ensemble average of amplitude and phase of a sequence of randomly scaled, IQ-demodulated pulses. Here we ignore quantization effects. We give the pdf of amplitude and phase modulation of complex signals in Gaussian noise, then discuss in which order ensemble averaging of IQ-demodulated and normalized signals should proceed (whether amplitude and phase should be computed for each individual pulse and then averaged or the average of *I* and *Q* should be used to compute phase and amplitude averages. See Fig. 4 for the two alternative methods). Then, we review the theory behind the optimal scaling threshold, which involves discarding pulses that have amplitudes below a certain threshold.

Consider the complex signal $Z(t)$ in terms of an IQ-decomposition; $Z(t) = I(t) + iQ(t)$. An IQ-demodulator provides a signal on this form in a sonar/radar or a radio. Alternatively, one may generate the quadrature signal by Hilbert transformation. To include random noise and scaling, we adopt the signal model

$$Z_k(t) = a_k Z_0(t) + n_k(t), \tag{7}$$

where t is time delay from pulse start and *k* is pulse number. The scaling a_k is accounted for by a general distribution $p(a)$, where a is a positive, real number. The noise is complex and Gaussian with variance σ^2 . We assume a certain noise correlation function with a characteristic correlation time that is sufficiently short such that noise in different pulses is uncorrelated. We will in the following consider the phase and amplitude modulations, which are

$$\begin{aligned} \phi_k(t) &= \mathrm{Arg}\left(Z_k(t)\right), \\ A_k(t) &= \mathrm{Mod}(Z_k(t)), \end{aligned} \tag{8}$$

respectively. Both these modulations have a random component due to noise and scaling.

3.1 Phase and amplitude statistics in general terms

The starting point to obtain the pdf's in question, is to consider how the scaled and subsequently normalised complex numbers

$$\hat{Z}_k(t) = Z_k(t)/a_k = Z_0(t) + \frac{n_k(t)}{a_k} \tag{9}$$

are distributed in the complex plane. It is obvious that the phase of $\hat{Z}_k$ is unaffected, and that the normalized amplitude is accounted for, by the scaling. The associated amplitude and phase distributions are obtained by considering the conditional distributions for given a_k, and then integrating over the scaling distribution $p(a)$.

We obtain the conditional distribution by using the scaled variance $(\sigma/a)^2$ in place of σ^2 in the phase distribution for a Gaussian complex variable of variance σ^2 (see Davenport and Root, 1958; Papoulis, 1965),

$$p(\phi;q,a) = \frac{\exp\left(-a^2 q\right)}{2\pi} + \frac{\sqrt{a^2 q}\cos(\phi)\exp\left(-a^2 q\sin^2(\phi)\right)}{\sqrt{4\pi}}\left[1 + 2\mathrm{Erf}\left(\sqrt{2a^2 q}\cos(\phi)\right)\right], \tag{10}$$

where $q = A_0^2/(2\sigma^2)$, and Erf denotes the usual error function. With given a, the normalised amplitude $\hat{A} = A/a$ obeys a Rician distribution (Davenport and Root, 1958; Papoulis, 1965) with variance $(\sigma/a)^2$ and amplitude parameter $A_0 = \mathrm{Mod}(Z_0)$,

$$p(\hat{A};A_0,\sigma,a) = a^2(\hat{A}/\sigma^2)\exp\left(-a^2(\hat{A}^2 + A_0^2)/2\sigma^2\right) I_0(a^2\hat{A}A_0/\sigma\ ). \tag{11}$$

Here, I_0 is the modified Bessel function of zero order.

Integration over $p(a)$ yields the phase and amplitude distributions

$$p(\phi_k;q) = \int_0^\infty p(\phi_k;q,a)p(a)\,da, \tag{12}$$

$$p(\hat{A}_k;A_0,\sigma) = \int_0^\infty p(\hat{A}_k;A_0,\sigma,a)p(a)\,da. \tag{13}$$

The variances σ_A^2 and σ_ϕ^2 can now be obtained by calculation of the second moments of $p(\hat{A}_k;A_0,\sigma)$ and $p(\phi_k;q)$.

3.2 Order of ensemble averaging

Averaging methods: There are two different ways of generating accurate phase and amplitude estimates by ensemble averaging (see Fig. 4):

- **Method I**, which refers to calculating phase and amplitude of ensemble averaged I/a and Q/a.
- **Method II,** which refers to calculating phase and amplitude of each individual realization of the pair (I/a,Q/a) before ensemble averaging.

In radar- or sonar-terms, Method I can be regarded as "coherent integration" and Method II as "incoherent integration", where "integration" is to be understood as ensemble averaging.

Method I: For sufficiently large ensemble N, the averages of the output of the IQ-demodulator $\bar{I}$ and $\bar{Q}$ tend to normal distributions (Gaussian random variables) by invoking the Central Limit Theorem from basic statistics. For normalized averaging, the joint distribution of $\bar{I}$ and $\bar{Q}$ is also symmetric. One can then immediately use the classical "Rician" probability distributions (10) and (11) for the amplitude and the phase, respectively, which apply to Gaussian and symmetric joint distributions. Then, for Method I, the pdf of the amplitude is of the form (11) with σ replaced by σ_N, where

$$\sigma_N^2 = \frac{\sigma^2}{N}\int_0^\infty \frac{p(a)}{a^2}\,da, \tag{14}$$

and the pdf of the phase is of the form (10) with q replaced by $q_N = A_0^2/(2\sigma_N^2)$.

Method II: In Method II we calculate the phase and the amplitude of each individual realization of the pair (I/a,Q/a), before ensemble averaging. The phase and amplitude modulations are estimated by performing an ensemble average (pulse to pulse average) over all available pulses. The ensemble averaged phase and amplitude are

$$\langle \phi(t) \rangle = \frac{1}{N}\sum_{k=1}^{N} \phi_k(t), \tag{15}$$

$$\langle A(t) \rangle = \frac{1}{N}\sum_{k=1}^{N} \frac{A_k(t)}{\overline{A_k}}, \tag{16}$$

where the amplitude ensemble average is normalized and $\overline{A_k}$ is the time averaged pulse amplitude for pulse k. We assume that $\overline{A_k}$ estimates a_k with sufficient accuracy such that we can neglect the stochastic component of $\overline{A_k}$ in the analysis. We note that $\overline{A_k}$ is the average instantaneous pulse amplitude over a single pulse k only. The pdfs of $\phi_k(t)$ and $A_k(t)/\overline{A_k}$ for fixed delay give the variance of the individual terms in the sum. The variance of the ensemble average is found by scaling this variance with $1/N$, since the individual terms are uncorrelated.

One can show that the joint pdf of (I/a,Q/a) is non-Gaussian. This can be handled by treating the Rician distributions as conditional distributions for given a, and then integrating over $p(a)$ to obtain the non-Rician amplitude and phase distributions (12, 13). The resulting variances can then be calculated numerically. Finally, the variances for the ensemble averages are obtained by scaling with $1/N$, using the assumption of uncorrelated realizations.

Large SNR: In the large SNR case, the phase variance for both methods tend to the same value for $A_0 \gg \sigma$: In this limit $a^2 q \gg 1$ (for not too small a), such that the phase pdf (12) for Method II can be replaced by a normal distribution (see Appendix A of Øyehaug & Skartlien, 2006) with variance

$$\sigma^2_{\phi,\mathrm{M2}} = \frac{(\sigma/A_0)^2}{N}\int_0^\infty \frac{p(a)}{a^2}da. \tag{17}$$

Similarly, the phase distribution for Method I has the variance $1/(2q_N)$ in the same limit, and it follows that $\sigma^2_{\phi,\mathrm{M1}} = \sigma^2_{\phi,\mathrm{M2}}$. We conclude that the two methods give different phase variance only for moderate signal to noise ratios, which means a low amplitude radar or sonar pulse, or on the rising and falling edges of the pulse in general.

Also the amplitude variance for both methods tend to the same value for $A_0 \gg \sigma$: In this limit, the amplitude distribution tends to a Gaussian near A_0. The integrand of the amplitude distribution in (13) is then a Gaussian with expectation $E[A;a] = A_0 + (\sigma/a)^2/(2A_0)$ and it can be shown that

$$\sigma^2_{A,\mathrm{M2}} = \frac{\sigma^2}{N}\int_0^\infty \frac{p(a)}{a^2}da. \tag{18}$$

Similarly, the amplitude distribution (11) for Method I has variance σ^2_N in the same limit. It then follows that $\sigma^2_{A,\mathrm{M1}} \to \sigma^2_{A,\mathrm{M2}}$ for $A_0/\sigma \to \infty$. We conclude that the two methods give different amplitude variances only for moderate signal to noise ratios.

Comparison of methods: Which of the two methods gives the smallest amplitude and phase variance for moderate signal to noise ratios? The answer is non-trivial, since the computation of amplitude and phase is nonlinear. We need to express how the variances depend on the noise, the signal amplitude and *N*. With the phase and amplitude pdfs (10) and (11), we obtain for Method I:

$$\begin{aligned}\sigma^2_{A,\mathrm{M1}} &= \sigma^2_{A,\mathrm{M1}}(A_0, [\sigma/A_0]^2/N),\\ \sigma^2_{\phi,\mathrm{M1}} &= \sigma^2_{\phi,\mathrm{M1}}([\sigma/A_0]^2/N).\end{aligned} \tag{19}$$

For Method II, we can assume that the terms in the averaging sum are uncorrelated, and obtain the usual $1/N$ -law,

$$\begin{aligned}\sigma^2_{A,\mathrm{M2}} &= \sigma^2_{A,\mathrm{M2}}(A_0, (\sigma/A_0)^2)/N,\\ \sigma^2_{\phi,\mathrm{M2}} &= \sigma^2_{\phi,\mathrm{M2}}([\sigma/A_0]^2)/N.\end{aligned} \tag{20}$$

The difference between the methods then arises when we scale the *argument* with $1/N$ in contrast to scaling the *variances* with $1/N$. Either way, the amplitude as well as the phase variance decrease with increasing *N*. Comparing the performance of Methods I and II then comes down to establishing which is the smallest of the functions $f_{\mathrm{M1}}(x/N)$ and $f_{\mathrm{M2}}(x)/N$, where $x = (\sigma/A_0)^2$ and the *f*'s express the phase variance or the amplitude variance. Thus, given the value of *N* we should be able to establish for which signal-to-noise ratios Method I is favourable over Method II and vice versa. One can expect that the differences between the variances of Method I and II vary as function of *N* and σ in general. Below, we quantify these differences for given signal strength and noise level by integrating over the pdf's, when an explicit form is not available.

Amplitude: There are two independent parameters in the amplitude pdf; A_0 and σ. We plot the output NSR as function of N (Fig. 5A) for σ = 1 and σ = 0.1. In the former case Method II performs best, in the latter the methods are virtually indistinguishable. The plot of output NSR as function of SNR (Fig. 5B) gives the same conclusion; Method II is the best choice, this time by a clear margin for both values of σ. For high SNR, however, the methods are indistinguishable; the variances for the two methods coalesce near SNR=10.

Phase: The variance of the phase depends only on the input SNR via $q = A_0^2 / (2\sigma^2)$. Fig. 5C displays the standard deviation of the phase as function of N (measured in degrees) for σ = 1 and σ = 0.1. For the former and for low values of N, Method II is the best, otherwise the methods have close to indistinguishable variances. Considering variation in input SNR (Fig. 5D), for low input SNR, Method I is the best, for moderate SNR, Method II is the best. The difference between the two methods converges rapidly to zero with increasing input SNR. In summary, Method II appears to achieve the smallest variances, the only exception being at low-to-moderate input SNR for the phase variance.

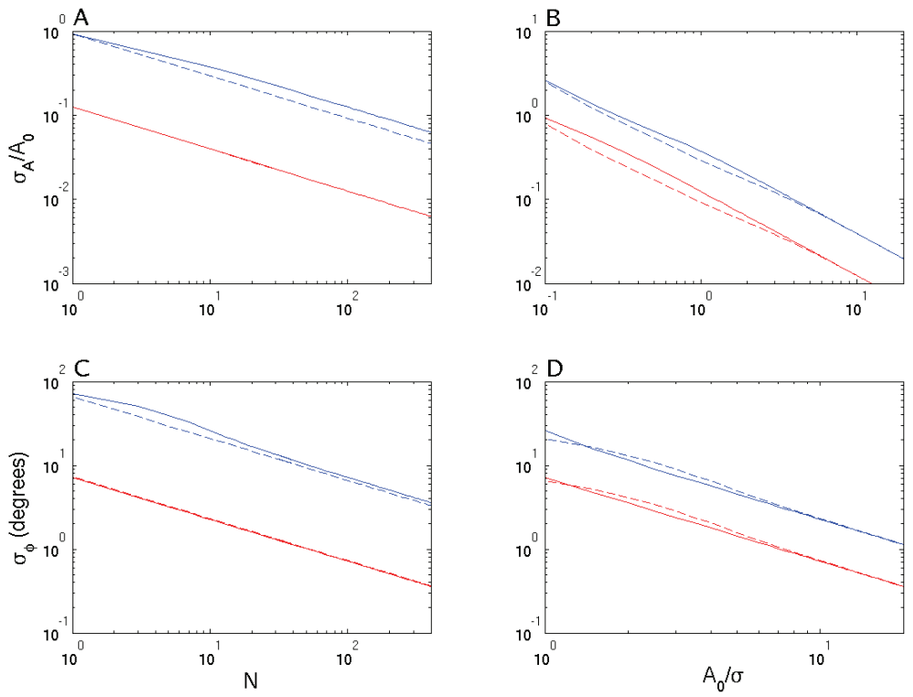

Fig. 5. Comparison of Method I and II. Output amplitude NSR σ_A/A_0 as function of (A) N and of (B) input SNR A_0/σ using Method I (solid line) and Method II (dashed) for σ = 1 (blue) and σ = 0.1 (red). Plots (C) and (D) display the same for the phase standard deviation (in degrees).

3.3 Optimum thresholding

In the preceding subsection we saw that when one considers moderate to good signal to noise ratios it is possible to obtain analytic, approximate expressions for the phase and amplitude variances (given in eqs. (17) and (18), respectively). Both these variances are proportional to the quantity

$$R = \frac{1}{N}\int_0^\infty \frac{p(a)}{a^2}\,da. \tag{21}$$

One can see the possibility of minimising R by rejecting pulses below a certain threshold a_0. A new truncated distribution $p(a;a_0)$ governs the remaining data and we obtain

$$R(a_0) = \frac{1}{n(a_0)}\int_{a_0}^\infty \frac{p(a)}{a^2}\,da, \tag{22}$$

where $n(a_0) = N\int_{a_0}^\infty p(a)\,da$ is the reduced ensemble size. A minimum point exists provided that $\int_{a_0}^\infty p(a)/a^2\,da$ decreases faster than $n(a_0)$ for small a_0, and slower than $n(a_0)$ for larger a_0. The existence and location for the optimal threshold depends entirely on the properties of $p(a)$. We find that a necessary condition for the existence of a minimum is (Øyehaug & Skartlien, 2006),

$$\int_{a_0}^\infty \left(\frac{a_{\min}}{a}\right)^2 p(a)\,da < \frac{1}{2}, \tag{23}$$

where $p(a)$ is the original distribution. Optimum thresholding is further investigated below in Sect. 4, where the signals are also assumed to be quantized.

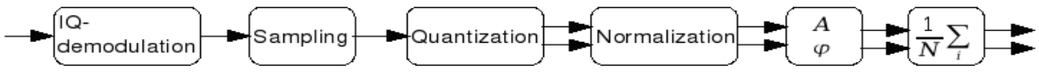

Fig. 6. The signal processing chain under consideration in Sect. 4. The input signal is demodulated into I and Q, sampled and quantized before it is normalized. The two components are then used to estimate amplitude and phase and finally the ensemble averages are computed using amplitude and phase from each individual pulse (Method II of Sect. 3).

4. Ensemble averaged randomly scaled amplitude and phase in quantized signals

This section considers the combination of the signal models that we looked at in Sects. 2 and 3, i.e. the signal under study has undergone IQ-demodulation, sampling, quantization, normalization, modulation into amplitude and phase and, finally, ensemble averaging (Fig. 6). The complex signal to be considered before modulation is

$$U_k(t) = \frac{1}{a_k}Q\big[Z_k(t)\big] = \frac{1}{a_k}Q\big[a_k Z_0(t) + n_k(t)\big]. \tag{24}$$

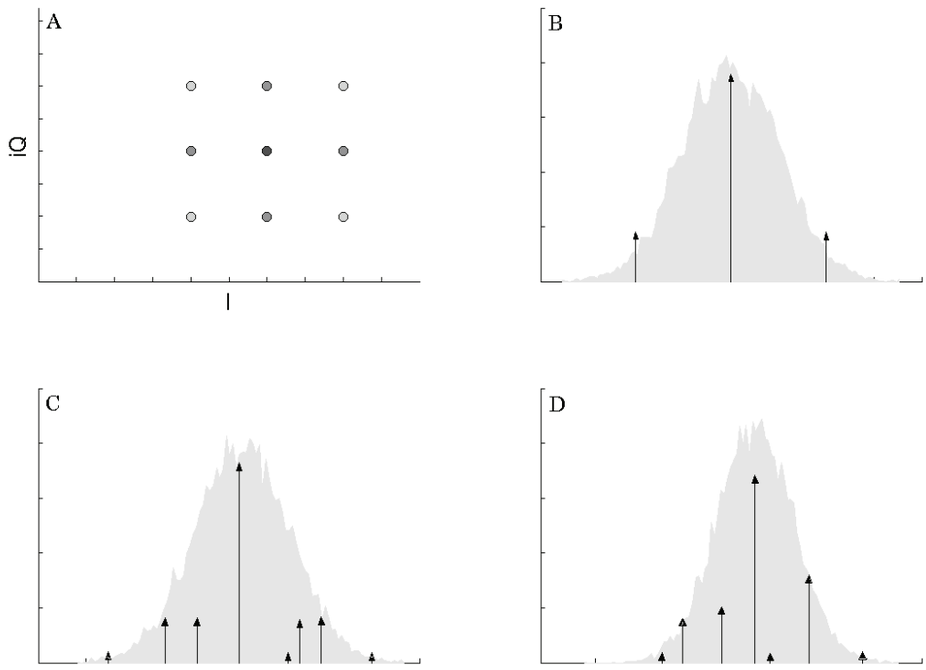

Fig. 7. (A) Typical distribution of the quantization of IQ-demodulated noisy signals in the complex (*I,Q*)-plane. The degree of shading of the markers indicates the frequency of each quantization level. (B) Histograms of the distribution (shaded) of noisy signals for *I* (the histogram for *Q* is similar), amplitude and phase (C, D). The associated discrete distributions of the quantized signal are depicted as arrows (not correctly scaled compared to the continuous distributions).

4.1 Statistical properties of randomly scaled and quantized complex signals

Due to quantization, the complex numbers in (24) follow a discrete pdf depicted as arrows in Fig. 7B where the normalized histogram of the Gaussian noise (corresponding to the pdf) is drawn for comparison. Deriving a general pdf for amplitude and phase that accounts for quantization as well as stochastic noise poses an extremely difficult mathematical problem that we do not attempt to solve. Instead we employ a mixture of graphical arguments and simulations to shed light on the statistics of these quantities.

In Fig. 7A there are nine possible complex values for the given noise and quantization levels, of which two have identical amplitude and two pairs of points have identical angle, which explains that there are eight different attainable values of the amplitude (Fig. 7C) and seven different for angle (Fig. 7D). We note that despite the low SNR in this example the underlying amplitude and phase pdfs (represented by shaded histograms in Figs. 7C, D) resemble very much Gaussian distributions.

We observe that the amplitude and phase pdfs when quantization is included, differ both qualitatively and quantitatively from the pdfs obtained when quantization is neglected. Despite this, the differences between the corresponding *variances* need not be as large as one

might expect when comparing the pdfs. For Gaussian noise and σ/Δ sufficiently large, eqs. (2) and (3) give the following approximate expression for the variance of a signal s_j with a given scaling a (not random);

$$\mathrm{Var}[e_{i,j};s_j,a] \simeq \frac{1}{a^2}\left(\frac{\Delta^2}{12}+\sigma^2-\left(\frac{\Delta}{\pi}\right)^2 \exp[-2\pi^2a^2(\sigma/\Delta)^2]\times \right.$$
$$\left.\left[\left(1+4\pi a^2(\sigma/\Delta)^2\right)\cos(2\pi s_j a/\Delta)+\exp[-2\pi^2a^2(\sigma/\Delta)^2]\sin^2(2\pi s_j a/\Delta)\right]\right). \quad (25)$$

With increasing σ/Δ the variance in (25) goes rapidly to $\left(\Delta^2/12+\sigma^2\right)/a^2$ such that the error variance becomes signal-independent. In Sect. 3.2 we argued that, in the large SNR limit and without taking into account quantization (i.e. Δ=0), this estimate also holds for the amplitude variance σ_A^2 and the phase variance multiplied by the squared signal amplitude $A_0^2\sigma_\phi^2$. Thus we expect, at least for small Δ, that eqs. (17) and (18) remain valid with σ^2 replaced by $\Delta^2/12+\sigma^2$. Among other things we examine this validity numerically in Sect. 4.2 below.

Consider random scaling with a uniform scaling pdf; $p(a)=1/(1-a_{\min})$ on $(a_{\min},1)$. The corresponding truncated pdf is $p(a;a_0)=1/(1-a_0)$ on $(a_0,1)$. Straightforward calculus applied to eqs. (15) and (16) establishes that, in the large SNR and σ/Δ limits,

$$\sigma^2_{\langle\phi\rangle}=\left(\frac{\sigma^2+\Delta^2/12}{A_0^2N}\right)\frac{1-a_{\min}}{a_0(1-a_0)},$$
$$\sigma^2_{\langle A\rangle}=\left(\frac{\sigma^2+\Delta^2/12}{N}\right)\frac{1-a_{\min}}{a_0(1-a_0)}. \quad (26)$$

These estimates are subject to numerical investigation below in Sect. 4.2.

4.2 Numerical results

Numerical experiments were performed to demonstrate the validity of the asymptotical estimates (26) and to examine the effect of quantization on thresholding. We estimated the variances numerically with a uniform $p(a)$, and compared these to the asymptotic values obtained analytically. The numerical results estimate the exact variances for all SNR, whereas the analytical results are valid only asymptotically for large SNR and σ/Δ.

The numerical variance estimates are based on a series of realizations of (24). We conducted the experiments as follows. Let $a_k, k=1,...,N$ be a random sequence where the elements are uniformly distributed on $(a_{\min},1)$, where $a_{\min}$ = 0.01. For a randomly selected Z_0 (see below), the complex numbers $Z_{k\ell}=a_{k\ell}Z_0+n_{k\ell}$ (where $n_{k\ell}$ is complex and Gaussian and the real and imaginary parts are independent) are computed for $k=1,...,N, \ell=1,...,M$, where k is the pulse index, while ℓ is a realization index. Different realizations are necessary for estimating the variances numerically. For each ℓ, we estimated the mean values $\langle A/\overline{A}\rangle$ and $\langle\phi\rangle$ by summing over k. The variances of these averages were estimated by summing over ℓ.

For convenience, the sequence in a_k is sorted according to increasing scaling to easily handle the thresholding. Each k then corresponds to a scaling threshold a_k. Only data with scaling $a \geq a_k$ were retained and used for signal estimation; for each value of k the mean values $\langle A / \overline{A} \rangle_{k\ell}$ and $\langle \phi \rangle_{k\ell}$ were computed including a_k for indices $k, k+1, ..., N$. Subsequently, amplitude and phase variance estimates were obtained by averaging over all realizations $\ell = 1, ..., M$;

$$\hat{\sigma}^2_{\langle \phi \rangle} = \frac{1}{M} \sum_{\ell=1}^{M} \left(\langle \phi \rangle_{k\ell} - \arg(Z_0) \right)^2 ,$$
$$\hat{\sigma}^2_{\langle A \rangle} = \frac{1}{M} \sum_{\ell=1}^{M} \left(\left\langle A / \overline{A} \right\rangle_{k\ell} - \mathrm{mod}(Z_0) \right)^2 . \quad (27)$$

The simulations were performed for three values of the quantization separation Δ. To avoid signal-dependent estimates, which is generally the case (see eq. 25), for each Δ we repeated the protocol described above 100 times with Z_0 selected at random on the circle in the complex plane with modulus 4 and thereafter calculated the mean variance estimate. Comparing the asymptotical expressions in (26) with the numerical results in Fig. 8, we observe that there is a reasonable agreement between numerical and theoretical estimates, with two notable exceptions: (i) for small values of a_0 and for large noise the numerical variances deviate markedly from the theoretical estimates and (ii) for large Δ and small noise (in particular for the phase variance), the numerical variances are clearly larger than the theoretical estimate.

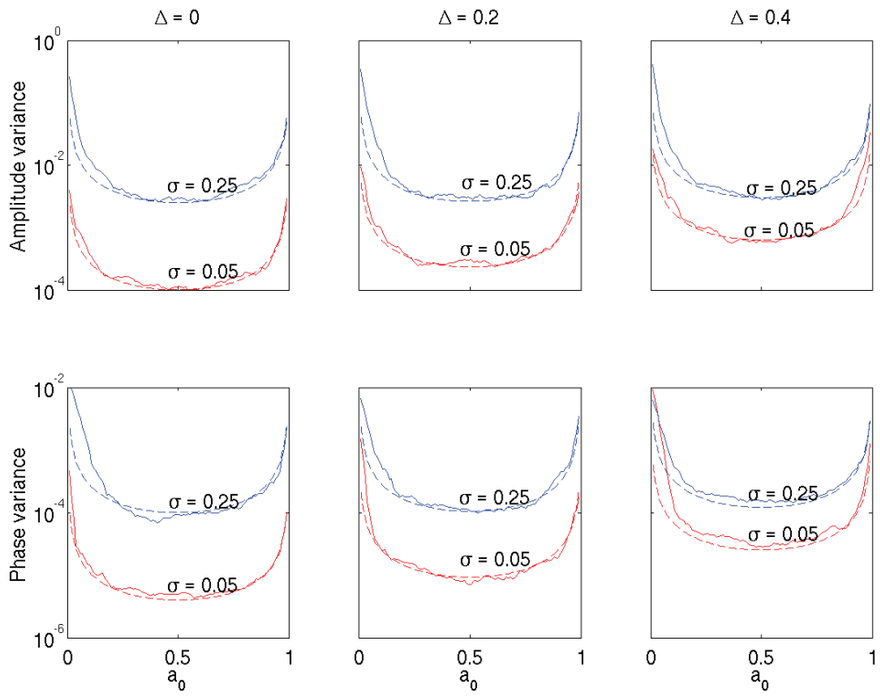

Fig. 8. Amplitude and phase variances as function of scaling threshold a_0 for the specified values of σ and Δ obtained by performing the computations described in the main text (solid lines) and corresponding asymptotical estimates (eqs. 26, dashed).

5. Discussion

As the test case in Sect. 4.2 shows, it was justified to apply the asymptotic estimates in Sect. 3 for both phase and amplitude averaging for sufficient levels of SNR ranging from roughly 10. Although this SNR is reasonable for many practical purposes, the instantaneous signal to noise ratio varies throughout the radar/sonar pulse with the instantaneous amplitude. Parts of the rising and falling flanks of the pulses will then correspond to short time intervals in which the theory should not be applied.

We adopted a smooth scaling distribution $p(a)$ in our analysis. In a practical situation, only the scaling histogram is available. The normalised histogram approximates $p(a;a_0)$ and the optimal scaling threshold can be obtained by the discrete analog to eq. (23). On the other hand, the optimum scaling threshold can of course be computed by brute force, i.e. by straightforward estimation of the variance based on available pulse signals and rejecting those pulses that contribute to a degraded ensemble average. One interesting possible future investigation is to evaluate the brute force and theoretically driven approaches in practical situations and compare them in terms of efficiency and reliability.

In Sect. 2.3 we defined and obtained a mathematical expression for the mean square error (MSE) of the ensemble average of a quantized, noisy signal. The MSE is a signal-independent measure of the average signal variance. When the signals over which we average are randomly scaled, there is no obvious way of defining the MSE. One way of circumventing this problem is to, as we did in Sect. 4.2 above, calculate variances of a large number of randomly selected points and then taking the average in order to achieve variances that are roughly signal-independent (Fig. 8). In the future, more sophisticated definitions of average variance that account for random scaling as well as quantization and stochastic noise should be developed.

Direct averaging with subsequent amplitude and phase calculation (Method I) provides the same results as Method II in the large SNR limit. Method I is potentially a more efficient averaging method, since amplitude and phase need not be computed for each pulse. However, signal degradation is more sensitive to alignment errors of the pulses before averaging; the sensitivity to precise alignment increases for increased carrier frequency due to larger phase errors for the same time lag error. This problem is much reduced when one performs averaging on amplitude and phase modulations directly (Method II).

6. Conclusion

We have reviewed the statistics of (i) averaged quantized pulses and (ii) averaged amplitude and phase modulated pulses that are randomly scaled, but not quantized. We showed that ensemble averaging should be performed on the amplitude and phase modulations rather than on I and Q. In the final point (iii), we analyzed the asymptotic statistics for ensemble averaged amplitude and phase modulated pulses that are both randomly scaled and quantized after IQ-demodulation. We studied the effect of thresholding (rejecting pulses below a certain amplitude) and found that theoretical estimates of the variance as function of threshold, closely agree with numerical estimates.

We believe that our analysis is applicable to radar and sonar systems that rely on accurate estimation of pulse characteristics. We have covered three key aspects of the problem, with the goal of reducing statistical errors in amplitude and phase modulations. Extensions or modifications of our work may be necessary to account for the signal chain in a specific digital system.

7. References

Ai, C. & Guoxiang, A. (1991). Removing the quantization error by repeated observation. *IEEE Trans. Signal Processing*, vol. 39, no. 10, (oct 1991) 2317-2320, ISSN: 1053-587X.

Belchamber, R.M. & Horlick, G. (1981). Use of added random noise to improve bit-resolution in digital signal averaging. *Talanta*, vol. 28, no 7, (1981) 547-549, ISSN: 0039-9140.

Carbone, P. & Petri, D. (1994). Effect of additive dither on the resolution of ideal quantizers. *IEEE Trans. Instrum. Meas.*, vol. 43, no 3, (jun 1994) 389-396, ISSN: 0018-5456.

Davenport, W.B. Jr. & Root, W.L. (1958), *An Introduction to the Theory of Random Signals and Noise*, McGraw-Hill Book Company, Inc., New York.

Jane, R. H., Rix, P., Caminal, P. & Laguna, P. (1991). Alignment methods for averaging of high-resolution cardiac signals - a comparative study of performance. *IEEE Trans. Biomed. Eng*, vol. 38, no. 6 (jun 1991) 571-579, ISSN: 0018-9294.

Koeck, P.J.B. (2001). Quantization errors in averaged digitized data. *Signal Processing*, vol. 81, no. 2, (feb 2001) 345-356, ISSN: 0165-1684.

Laguna, P. & Sornmo, L. (2000). Sampling rate and the estimation of ensemble variability for repetitive signals. *Med. Biol. Eng. Comp*, vol. 38, no. 5, (sep 2000) 540-546, ISSN: 0140-0118.

Meste, O. & Rix, H. (1996). Jitter statistics estimation in alignment processes. *Signal Processing*, vol. 51, no. 1, (may 1996) 41-53, ISSN: 0165-1684.

Øyehaug, L. & Skartlien, R. (2006). Reducing the noise variance in ensemble-averaged randomly scaled sonar or radar signals. *IEE Proc. Radar Sonar Nav.,* vol. 153, no. 5, (oct 2006) 438-444, ISSN: 1350-2395.

Papoulis, A. (1965). *Probability, Random Variables, and Stochastic Processes*, McGraw-Hill Book Company, Inc., New York, ISBN: 0-07-048448-1.

Schijvenaars, R.J.A., Kors, J.A. & Vanbemmel, J.H. (1994). Reconstruction of repetitive signals. *Meth. Inf. Med.*, vol. 33, no. 1, (mar 1994) 41-45, ISSN: 0026-1270.

Skartlien, R. & Øyehaug, L. (2005). Quantization error and resolution in ensemble averaged data with noise. *IEEE Trans. Instrum. Meas.*, vol. 53, no. 3, (jun 2005) 1303-1312, ISSN: 0018-5456.

Viciani, S., D'Amato, F., Mazzinghi, P., Castagnoli, F., Toci, G. & Werle, P. (2008). A cryogenically operated laser diode spectrometer for airborne measurement of stratospheric trace gases. *Appl. Phys. B*, vol. 90, no. 3-4, (mar 2008), 581-592, ISSN: 0946-2171.

Advances in Sonar Technology

Edited by Sergio Rui Silva

ISBN 978-3-902613-48-6
Hard cover, 450 pages
Publisher I-Tech Education and Publishing
Published online 01, February, 2009
Published in print edition February, 2009

The demand to explore the largest and also one of the richest parts of our planet, the advances in signal processing promoted by an exponential growth in computation power and a thorough study of sound propagation in the underwater realm, have lead to remarkable advances in sonar technology in the last years.The work on hand is a sum of knowledge of several authors who contributed in various aspects of sonar technology. This book intends to give a broad overview of the advances in sonar technology of the last years that resulted from the research effort of the authors in both sonar systems and their applications. It is intended for scientist and engineers from a variety of backgrounds and even those that never had contact with sonar technology before will find an easy introduction with the topics and principles exposed here.

InTech Europe
University Campus STeP Ri
Slavka Krautzeka 83/A
51000 Rijeka, Croatia
Phone: +385 (51) 770 447
Fax: +385 (51) 686 166
www.intechopen.com

InTech China
Unit 405, Office Block, Hotel Equatorial Shanghai
No.65, Yan An Road (West), Shanghai, 200040, China
中国上海市延安西路65号上海国际贵都大饭店办公楼405单元
Phone: +86-21-62489820
Fax: +86-21-62489821

IntechOpen